Journal of Virology

Microbial Pathogenesis | Full-Length Text

PB2 residue 473 contributes to the mammalian virulence of H7N9 avian influenza virus by modulating viral polymerase activity via ANP32A

Miaomiao Zhang,[1,2] Mingbin Liu,[1] Hongjun Chen,[2] Tianyi Qiu,[3] Xuanxuan Jin,[4] Weihui Fu,[1] Qiaoyang Teng,[2] Chen Zhao,[1] Jianqing Xu,[1,3] Zejun Li,[2] Xiaoyan Zhang[1,3]

AUTHOR AFFILIATIONS See affiliation list on p. 17.

ABSTRACT Since the first human infection reported in 2013, H7N9 avian influenza virus (AIV) has been regarded as a serious threat to human health. In this study, we sought to identify the virulence determinant of the H7N9 virus in mammalian hosts. By comparing the virulence of the SH/4664 H7N9 virus, a non-virulent H9N2 virus, and various H7N9-H9N2 hybrid viruses in infected mice, we first pinpointed PB2 as the primary viral factor accounting for the difference between H7N9 and H9N2 in mammalian virulence. We further analyzed the *in vivo* effects of individually mutating H7N9 PB2 residues different from the closely related H9N2 virus and consequently found residue 473, alongside the well-known residue 627, to be critical for the virulence of the H7N9 virus in mice and the activity of its reconstituted viral polymerase in mammalian cells. The importance of PB2-473 was further strengthened by studying reverse H7N9 substitutions in the H9N2 background. Finally, we surprisingly found that species-specific usage of ANP32A, a family member of host factors connecting with the PB2-627 polymorphism, mediates the contribution of PB2 473 residue to the mammalian adaption of AIV polymerase, as the attenuating effect of PB2 M473T on the viral polymerase activity and viral growth of the H7N9 virus could be efficiently complemented by co-expression of chicken ANP32A but not mouse ANP32A and ANP32B. Together, our studies uncovered the PB2 473 residue as a novel viral host range determinant of AIVs via species-specific co-opting of the ANP32 host factor to support viral polymerase activity.

IMPORTANCE The H7N9 avian influenza virus has been considered to have the potential to cause the next pandemic since the first case of human infection reported in 2013. In this study, we identified PB2 residue 473 as a new determinant of mouse virulence and mammalian adaptation of the viral polymerase of the H7N9 virus and its non-pathogenic H9N2 counterparts. We further demonstrated that the variation in PB2-473 is functionally linked to differential co-opting of the host ANP32A protein in supporting viral polymerase activity, which is analogous to the well-known PB2-627 polymorphism, albeit the two PB2 positions are spatially distant. By providing new mechanistic insight into the PB2-mediated host range determination of influenza A viruses, our study implicated the potential existence of multiple PB2-ANP32 interfaces that could be targets for developing new antivirals against the H7N9 virus as well as other mammalian-adapted influenza viruses.

KEYWORDS H7N9, PB2, host specificity, virulence, viral polymerase activity, ANP32A

Novel H7N9 avian influenza virus (AIV) has continued to be a public threat since the first case of human infection reported in March 2013. As of April 2020, the identified cases of human infections caused by H7N9 AIVs had reached 1,568, including at least

Editor Anice C. Lowen, Emory University School of Medicine, Atlanta, Georgia, USA

Address correspondence to Xiaoyan Zhang, zhangxiaoyan@fudan.edu.cn, Zejun Li, lizejun@shvri.ac.cn, Jianqing Xu, xujianqing@fudan.edu.cn, or Chen Zhao, chen_zhao72@163.com.

Miaomiao Zhang and Mingbin Liu contributed equally to this article. Author order was determined on the basis of strength of contribution.

The authors declare no conflict of interest.

Received 14 December 2023
Accepted 14 February 2024
Published 29 February 2024

617 deaths (http://www.who.int/influenza). Genetically, the H7N9 AIV from 2013 is a reassortant virus with six internal gene segments contributed by H9N2 viruses circulating in poultry (1, 2).

In order to infect mammals, AIVs need to cross species barrier. This barrier is created by virus's dependence on cellular machinery to replicate and the genetic diversity between different host species. The pro-viral factors used by AIVs in avian cells could be different in mammalian cells; thus, only virus variants developing adaptive mutations that enable the co-opting of mammalian co-factors could establish effective viral production and transmission in mammalian context(s). A best example is provided by the human adaptation of viral haemagglutinin (HA) surface protein, which mediates viral entry by binding to sialic acid (SA) on the surface of host cells. Although avian- and mammalian-type HAs both recognize sialic acid, they show different receptor preference: the former preferentially recognize α2,3-linked SA whereas the latter have higher affinity for α2,6-linked SA, which is highly expressed in the upper respiratory tract of human (3) . A switch of receptor specificity of HA is widely regarded as a prerequisite for human spillover of AIV, as evidenced by the characterization of receptor specificity-changing residues in the HAs expressed by some of the 20th century pandemic influenza strains (4). The HA of novel H7N9 AIVs could, to some extent, recognize the α2,6-linked SA (5), possibly underlying their ability to cause human infections with relatively high frequency.

Besides HA, PB2 is the other major viral protein with a determining role in host specificity. As one of the three subunits of the influenza's polymerase complex , PB2 harbors multiple residues whose changes are associated with the adaptation of AIV to human, best known for the 627 position. In contrast to bird-derived isolates of AIVs, whose PB2s almost exclusively feature a glutamic acid at the 627 position (PB2-627E), PB2s of human-derived isolates often show a mutation to lysine at this position (PB2-E627K) (6–9). Functional studies revealed that PB2-E627K conversion markedly enhances the activity of polymerase of AIV and consequently leads to enhanced viral growth in mammalian cells, an effect not observed within the avian context (7, 10). Intriguingly, some mammalian influenza A viruses (IAVs) of non-human origin do not have PB2-627K but contain other PB2 mutations that can functionally compensate for the absence of E627K mutation. PB2-D701N leads the list of these mutations, followed by K526R, Q591K, and others (11–13).

The host factors underpinning the association between PB2-627K/E polymorphism and host specificity of IAVs were recently identified as proteins belonging to the acidic nuclear phosphoproteins of 32 kilodaltons (ANP32) family (14). Consisting of three members in ANP32A, ANP32B, and ANP32E, the ANP32 family is characterized by the possession of a N-terminal domain comprising five leucine-rich repeats (LRRs) and a C-terminal low complexity acidic region (LCAR), which are connected by a short linker region referred to as the "central domain" (14). A remarkable characteristic of ANP32A is the regulation of its mRNA by species-dependent alternative splicing: most avian species predominantly express a relatively longer form with a 33-amino acid insertion into the central domain; in contrast, mammalian species feature a shorter form missing such insertion (15, 16). The identity of ANP32A as a restricting factor for mammalian adaptation of IAVs was demonstrated by that co-expression of avian ANP32A, but not its mammalian counterpart, could restore the activity of viral polymerase with avian PB2-627E signature in mammal cells. This rescuing effect was attributed to the aforementioned 33-amino acid insertion (16). Recent studies further uncovered other divergence between as well as within birds and mammals in the usage of ANP32 proteins to support the polymerase activity of IAV. For example, such supporting activity was provided for PB2-627K-type IAV polymerase in human cells through both ANP32A and ANP32B, while only through ANP32A in mouse cells (17). Contrastingly, ANP32A is the only ANP32 protein co-opted by IAV polymerase in avian cells (17). There is evidence that the inherent difference in the splicing pattern of ANP32A constitutes a driving force for the evolution of AIVs within the natural avian repertoire, rendering them pre-adaptive to

mammalian hosts (18). The connection between ANP32A and IAV evolution was further strengthened by the unique capability of swine ANP32A to support the polymerase activity of the AIV type, in line with the labeling of pig as a mixed vessel that, owing to the susceptibility to infections of both avian and human IAVs, facilitates the creation of new reassorted virus more likely to cause pandemic than the parental strains (19).

Establishing a partnership with human ANP32 could not be the whole story underlying a variety of human adaptation mutations of PB2. Indeed, before ANP32A identification, the co-opting of mammalian importin-α proteins has been proposed as a mechanism responsible for the enhancing effect of PB2-D701N on the AIV polymerase activity in mammal cells (20). However, how exactly importin-α proteins impact the IAV polymerase activity remains unclear.

In this study, we sought to explore further the genetic and molecular bases of the mammalian virulence of H7N9 AIV. Specifically, we chose two H9N2 AIVs as low-pathogenic counterparts of H7N9 and generate a series of H7N9-H9N2 hybrid viruses. By comparing the infection outcomes of these reassorted viruses alongside the parental strains in mice, we identified the PB2 gene as the major determinant for differential mammalian virulence between the H7N9 and H9N2 viruses. We subsequently pinpointed 473M as the key residue besides 627K supporting the functionality of H7N9 PB2 in mammalian hosts. Mechanistically, we found that the decreasing effect of PB2-M473T mutation on the H7N9 polymerase activity in mammalian cells could be rescued by the co-expression of chicken ANP32A but not mouse ANP32A or ANP32B. Taken together, our data suggest that the PB2 473 residue is a new host range determinant of AIVs with a role in co-opting host ANP32 protein(s) shared by the PB2 627 residue.

RESULTS

Viral polymerase complex is the key mammalian virulence determinant of H7N9 AIV

To study the viral determinants of mammalian virulence of H7N9 virus, we selected two viruses identified in China, namely, H7N9 SH/4664 strain and H9N2 avian strain CK/F98, as backbones to generate hybrid viruses by reverse genetics for comparison in a mouse infection model. We have previously shown that grafting the six internal genes but not the two surface genes of H7N9 SH/4664 into CK/F98 resulted in a marked increase in pathogenicity and replication in mice, accompanied by enhanced viral growth in cultured human cells (21). Following that work, we replaced viral polymerase complex genes (PB2/PB1/PA/NP) or surface genes (HA alone or plus NA) of the H7N9 virus with those of the H9N2 virus (1, 21). The thus-generated recombinant viruses, namely, SH/4664-F98Vpol, SH/4664-F98HA, and SH/4664-F98HA/NA (Fig. 1A), were used individually for mice infection via intranasal inoculation at a dose of 10^6 50% egg infectious dose (EID_{50}) and compared with the parental H7N9 SH/4664 virus in terms of susceptibility and viral load. Mice showed high susceptibility to SH/4664-F98HA or SH/4664-F98HA/NA, indicated by both rapid weight loss during the first 6 days post infection (d.p.i.), comparable to SH/4664-challenged mice, and high lethality rate (60% and 80%, respectively) (Fig. 1B and D). Interestingly, there were also indications that F98HA and F98HA/NA replacements moderately attenuated the pathogenicity of SH/4664: the nadir of the weight of SH/4664-F98HA- or SH/4664-F98HA/NA-infected group appeared to be higher than that of the SH/4664-infected group; only the SH/4664-infected group exhibited 100% mortality on the 7 d.p.i. (Fig. 1D). In contrast, the SH/4664-F98Vpol-infected group did not experience weight loss, and all survived at the end of the 14-day observation period (Fig. 1B and D). The assessments of viral loads of lung and nasal turbinate at 4 d.p.i. were consistent with the susceptibility data, showing comparable viral loads among SH/4664-F98HA-, SH/4664-F98HA/NA-, and SH4664-infected groups, which were significantly higher than that observed with SH/4664-F98Vpol-infected mice (Fig. 1F). Collectively, these data pinpointed polymerase genes as the primary determinant accounting for the higher pathogenicity and replication capability of the

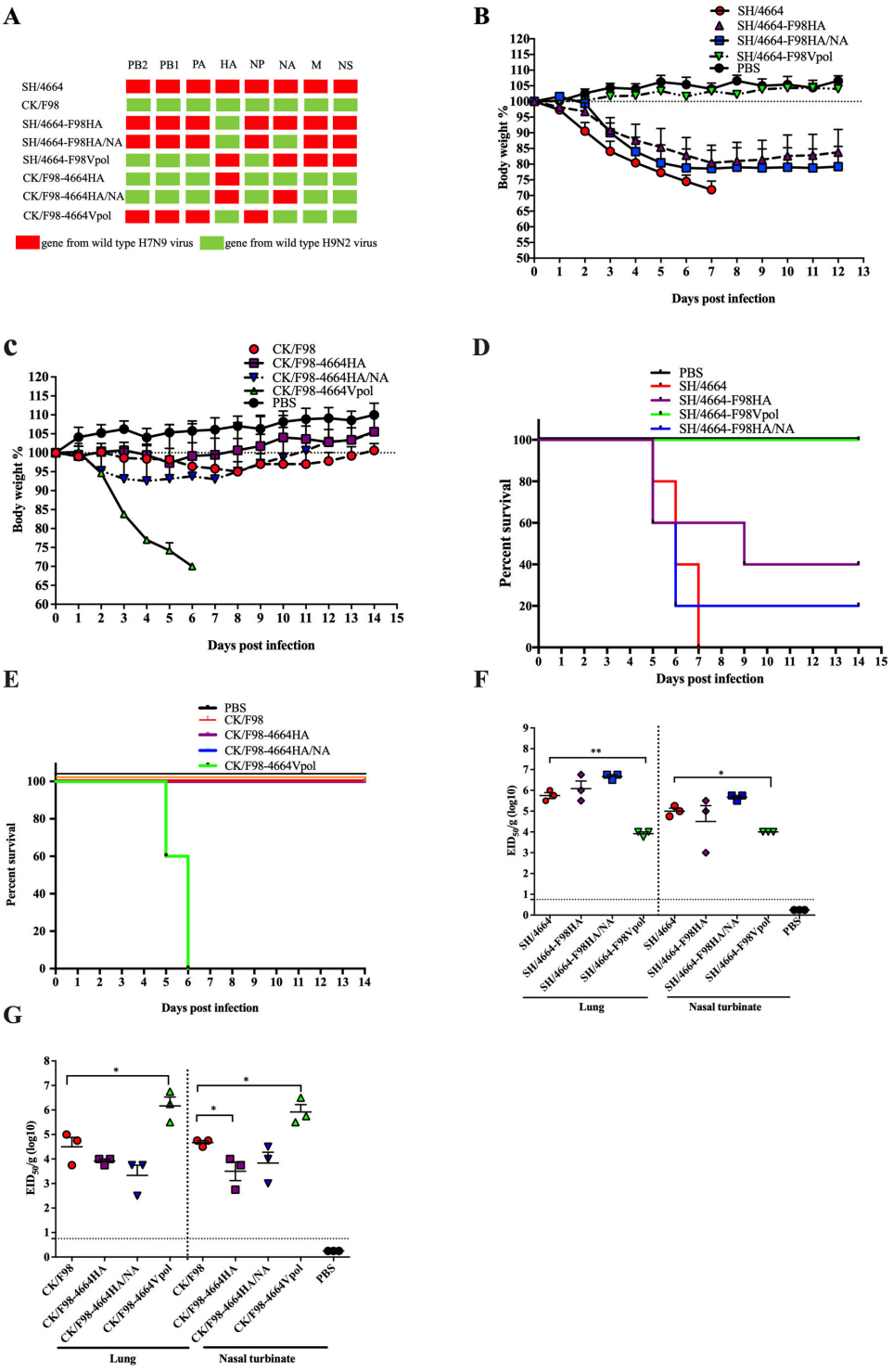

FIG 1 Viral polymerase complex genes, but not surface genes, contributed to the superior virulence of SH/4664 H7N9 over CK/F98 H9N2 in mice. Mice were intranasally inoculated with a single dose of 10^6 EID_{50} of the indicated H7N9-H9N2 hybrid virus, named after the virus backbone and the carried gene replacement joined by a hyphen, or the parental H7N9/H9N2 virus. The gene segment compositions of the used viruses were collectively shown in A. The infected mice were split into two groups. One group (n = 5) was subjected to daily monitoring of body weight changes (B and C) and mortality (D and E) until 12–14 days post the virus challenge. The other group (n = 3) was sacrificed on day 4 post infection for collecting lungs and nasal turbinates to make homogenates subjected to EID_{50} viral titer determination using embryonated chicken eggs (F and G). The dashed lines indicate the limit of detection of the assay; error bars represent the standard deviations. Statistical significance was analyzed using one-way ANOVA. *P < 0.05 and **P < 0.01.

SH/4664 H7N9 virus in mice than the CK/F98 H9N2 virus, with a minor contribution from the surface proteins.

Next, we examined whether the polymerase genes of SH4664 H7N9 are sufficient for conveying mammalian virulence to H9N2 AIV. To this end, we generated three additional H7N9-H9N2 reassortment viruses, designated as CK/F98-4664HA, CK/F98-4664HA/NA, and CK/F98-4664Vpol (Fig. 1A), by replacing the HA, HA plus NA, and the polymerase genes of CK/F98 H9N2 with the respective SH/4664 H7N9 analog(s). When examined in mice using the same infection condition as described above, only CK/F98-4664Vpol virus showed significantly enhanced susceptibility and viral loads as compared with the parental H9N2 virus (Fig. 1C, E and G). Thus, the sufficiency examination corroborated the necessity examination, implicating that one or more polymerase genes account for the superior mammalian fitness of the H7N9 virus over the H9N2 virus.

PB2 is the key viral determinant of mammalian virulence of the H7N9 virus

To assess the individual contribution of the three polymerase genes (PA, PB1, and PB2) to the mammalian pathogenicity of the H7N9 virus, we replaced the polymerase gene of SH/4664 H7N9 virus individually with that of CK/F98 H9N2 virus to generate three hybrid viruses, abbreviated as SH/4664-F98PB2, SH/4664-F98PB1, and SH/4664-F98PA (Fig. 2A). Given the critical role of viral NP protein in viral genome replication as an integral part of viral ribonucleoprotein (vRNP) besides polymerase, we also engineered an NP-swapped recombinant virus, SH/4664-F98NP (Fig. 2A). We subsequently compared the virulence of the four viruses in mice. Although the other three F98 replacements, particularly of PA and NP, also attenuated the pathogenicity of SH/4664, the F98PB2 replacement showed the most dramatic effect, nearly completely preventing the weight loss and allowing complete survival during the observation period (Fig. 2B and D). Corroborating such severely attenuated pathogenicity, the viral titers in the lungs and nasal turbinates of SH/4664-F98PB2-infected mice showed marked reduction compared with those of SH/4664-infected mice (Fig. 2F).

Next, we introduced a single polymerase or NP gene of SH/4664 H7N9 into the CK/F98 H9N2 backbone, resulting in four recombinant viruses, namely, CK/F98-4664PB2, CK/F98-4664PB1, CK/F98-4664PA, and CK/F98-4664NP (Fig. 2A). When examined in the mouse infection model as described above, CK/F98-4664PB2 showed markedly enhanced virulence compared with the CK/F98 parent: the body weights of CK/F98-4664PB2-infected mice were rapidly lost, reaching a nadir at 6 d.p.i and maintained at the same level until day 9 before starting gradual recovery in a small portion of animals, in line with approximately 80% lethality (Fig. 2C and E). Among the other three recombinant viruses, only CK/F98-4664NP showed a detectably increased pathogenicity, with infected mice suffering from weight loss but not lethality and the weight loss being less than that of the CK/F98-4664PB2 infection group (Fig. 2C and E). The significant gain of pathogenic traits in CK/F98-4664PB2 was consistent with substantially enhanced viral loads (Fig. 2G). Collectively, these studies led us to conclude that among the four viral proteins involved in the viral genome replication and transcription, PB2 is the primary determinant of higher mammalian virulence of the H7N9 virus compared with the H9N2 virus, with minor contributions from NP and PA.

We further assessed the roles of polymerase or NP gene in the pathogenicity of the H7N9 virus using another avian H9N2 virus, A/Chicken/Shanghai/A2093/2011 (CK/A2093), as a comparison. CK/A2093 was isolated in China 2 years earlier than SH/4664 and is considered the closest H9N2 strain relative identified so far to the SH/4664 virus. Four SH/4664 recombinant viruses were generated, each carrying a polymerase gene or NP gene from CK/A2093 (Fig. 3A). Among the four recombinant viruses, the SH4664-A2093PB2 virus with CK/A2093 PB2 caused essentially no body weight change in infected mice compared with the PBS control (Fig. 3B), allowing complete survival during the 14-day observation period (Fig. 3C). In contrast, replacement of PB1 with the CK/A2093 counterpart minimally affected the pathogenicity, whereas switching to CK/A2093 PA and NP showed a moderate impact on the survival rate, which could be attributed to

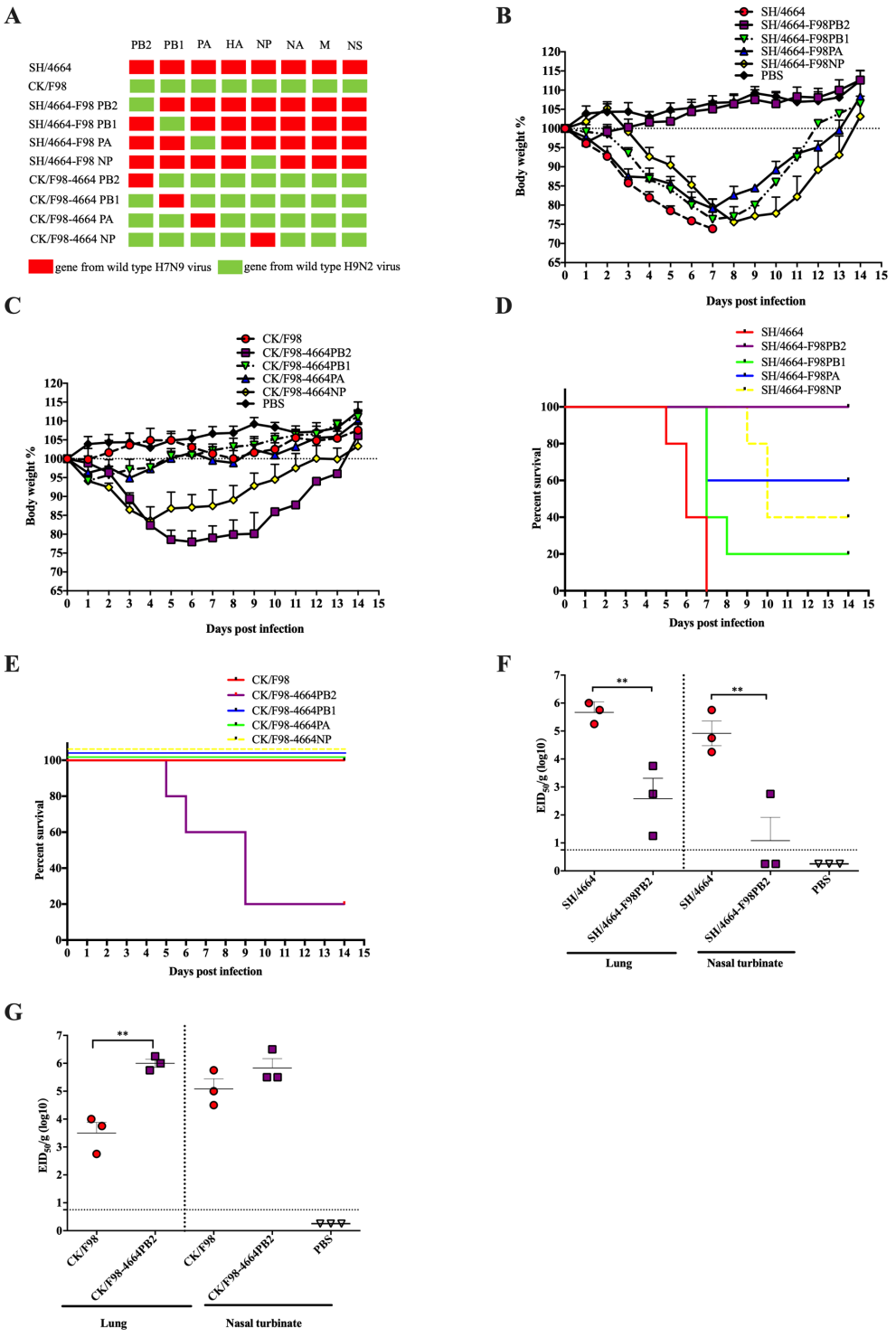

FIG 2 PB2 is the key viral gene determining the replication and pathogenicity of SH/4664 H7N9 versus CK/F98 H9N2 in mice. Mice were intranasally inoculated with the indicated SH/4664-CK/F98 hybrid virus or the parental virus, named similarly as in Fig. 1 with the gene segment composition shown in A, at a single dose of 10^6 EID_{50}. Shown are (B and C) body weight curves, (D and E) mortality curves, and (F and G) EID_{50} viral titers of lung and nasal turbinate assessed on 4 d.p.i. The dashed lines indicate the limit of detection, and the error bars represent the standard deviations. Statistical significance was analyzed using one-way ANOVA. *$P < 0.05$ and **$P < 0.01$.

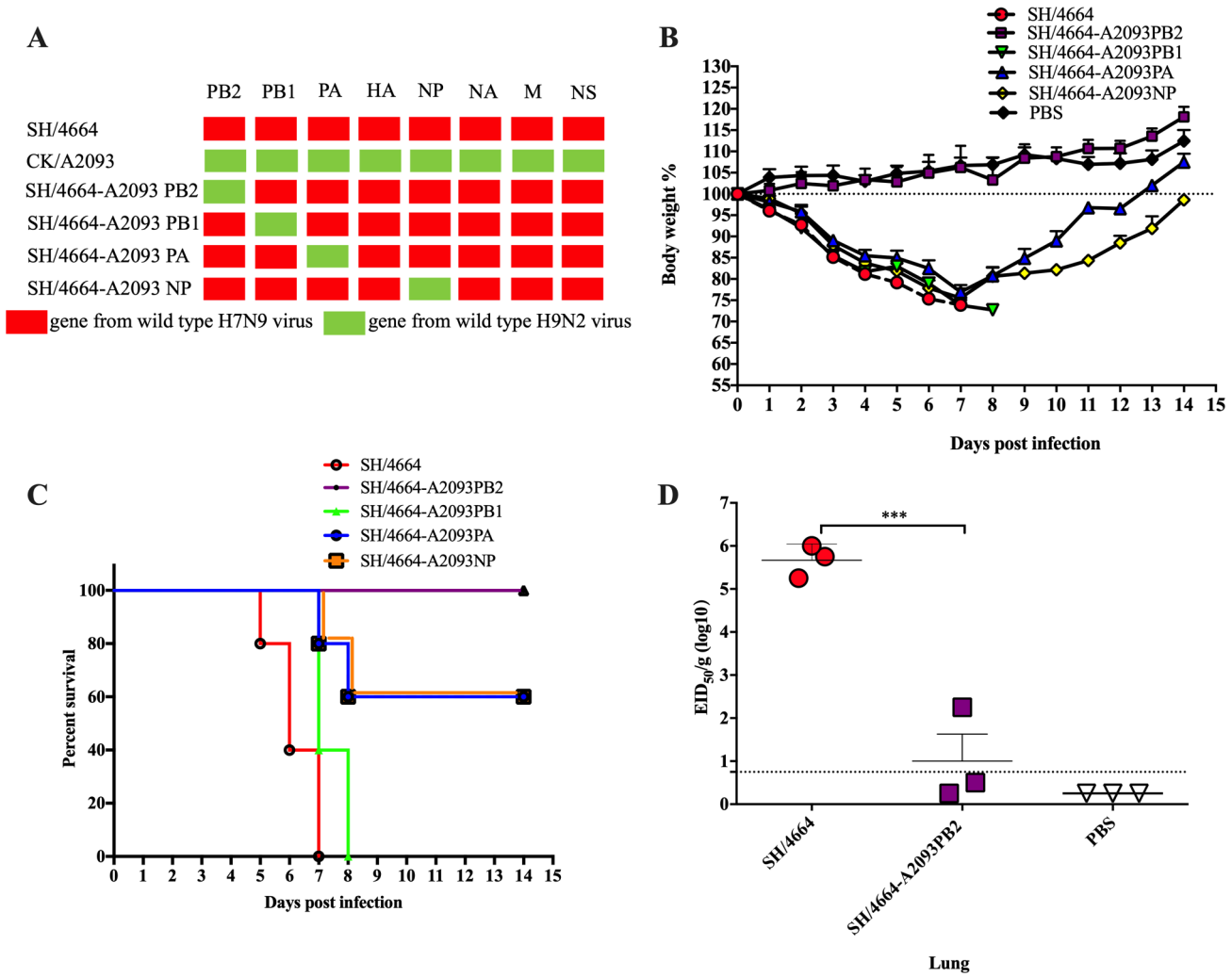

FIG 3 PB2 gene is the general determinant underlying the advantage of SH/4664 H7N9 over avian H9N2 in mouse infection. Mice were intranasally inoculated with PBS or a single dose of 10^6 EID_{50} of the wild-type SH/4664 virus or each of the four recombinant SH/4664 viruses, in which the three viral polymerase genes or NP gene was individually replaced by the counterpart of CK/A2093. Shown are (A) gene segment compositions of the used viruses, (B) body weight curves, (C) mortality curves, and (D) lung viral titers assessed at 4 d.p.i. The dashed line indicates the limit of detection of the assay; error bars represent the standard deviations. Statistical significance was analyzed using one-way ANOVA. *P < 0.05 and ***P < 0.001.

a late body weight recovery after days 7–8 post infection (Fig. 3B and C). Corroborating the pathogenicity data, the average viral lung load of the SH4664-A2093PB2-infected group was >4,000-fold lower than that of the SH/4664-infected group (10 EID_{50}/g versus 4.68×10^5 EID_{50}/g) (Fig. 3D). Thus, PB2 appears to be the common primary viral determinant separating H7N9 virus from H9N2 virus in mouse virulence. In other words, the evolution of the PB2 gene is potentially a required key step for H7N9 AIV to adapt to mammalian hosts.

M473 is a novel PB2 residue critical for the mammalian adaptation of H7N9 IAV through supporting viral polymerase activity

We next sought to identify key residues responsible for the differential ability of CK/A2093 PB2 and SH/4664 PB2 to support mouse virulence in the context of SH/4664 virus. Thus, we compared the PB2 coding sequences of SH/4664 and CK/A2093 viruses, finding a total of four amino changes that include a lysine (K)-to-glutamic acid(E) change at residue 191, a methionine (M)-to-threonine (T) change at residue 473, an asparagine (N)-to-T change at residue 559, and a K-to-E change at residue 627. We thus generated

four SH/4664 mutant viruses, each carrying a single PB2 residue change found in CK/A2093, namely, SH/4664-PB2-K191E, SH/4664-PB2-M473T, SH/4664-PB2-N559T, and SH/4664-PB2-K627E, and subsequently compared their virulence to that of wild-type SH/4664 in mice. Consistent with the above results, SH/4664-infected mice suffered from rapid weight loss starting from 1 d.p.i., reaching the sacrifice point by 6 d.p.i. (Fig. 4A). Confirming the identity of PB2-672K as a prominent mammalian adaptive mutation, the mice infected with the SH/4664-PB2-K627E virus only underwent mild weight loss while showing recovery after 7 d.p.i. Interestingly, similar relief of weight loss was also observed for the mice receiving the SH/4664-PB2-M473T virus except that those mice experienced more weight loss on 2–4 d.p.i. with the extent still markedly lower than the SH/4664-infected group (Fig. 4A). The body weight change data were corroborated by mortality and viral load measurements. In contrast to the SH/4664 H7N9-infected group showing 100% lethality by 7 d.p.i., the entire group of the SH/4664-PB2-M473T- and SH/4664-PB2-K627E-infected mice survived by the end of the 14-day observation period (Fig. 4B). Unlike PB2-M473T and PB2-K627E mutations, neither PB2-K191E nor N559T mutation showed a significant attenuating effect on the mouse pathogenicity of SH/4664 in terms of body weight loss or mortality (Fig. 4A and B). We further assessed the consequences of PB2-M473T and PB2-K627E mutations on virus replication. As measured at 4 d.p.i., SH/4664-PB2-M473T and SH/4664-PB2-K627E replicated to titers in the lungs that were approximately 1.7 and 2.6 logs lower than the wild-type SH/4664 virus, respectively ($P < 0.05$; Fig. 4C). A similar trend was observed for nasal turbinate titers ($P < 0.05$; Fig. 4D). In an independent mouse infection experiment, we further verified the attenuations in mouse virulence of the SH/4664-PB2-M473T virus and the SH/4664-PB2-K627E virus (Fig. S1). Collectively, these results demonstrated that both PB2 627K and 473M residues are required for mouse virulence of the SH/4664 virus.

We next assessed the impact of the PB2 M473T mutation on viral growth of the SH/4664 H7N9 virus in cultured mammalian cells. To this end, we infected MDCK cells with SH/4664-PB2-M473T, SH/4664-PB2-K627E, or the parental SH/4664 virus at a MOI of 0.001 and measured virus titers in the supernatants at different time points post infection. Consistent with the observations made in the mouse infection model, the SH/4664-PB2-M473T and SH/4664-PB2-K627E mutant viruses demonstrated significantly lower viral replication than the wild-type SH/4664 virus at all the time points examined ($P < 0.001$; Fig. 4E). We then used a minigenome assay to evaluate the effects of the PB2 M473T and K627E mutations on the activity of viral polymerase of SH/4664. As shown in Fig. 4F, the M473T mutation markedly decreased the viral polymerase activity, with the magnitude of the reduction (~17-fold) only slightly lower than that caused by the K627E mutation. Together, these results demonstrated that PB2-473M, analogous to PB2-627K, is required for effective replication of the SH/4664 H7N9 virus in mammalian cells because of its critical role in supporting viral polymerase activity.

We further examined the roles of PB2-473 and PB2-627 in the context of the CK/A2093 H9N2 virus. To this end, we generated three CK/A2093 mutant viruses with PB2-473 and PB2-627 individually or simultaneously changed to the corresponding residues of the SH/4664 H7N9 virus, designated as CK/A2093-PB2-E627K, CK/A2093-PB2-T473M, and CK/A2093-PB2-double-mut viruses, and then examined them in a mouse infection model compared with the wild-type CK/A2093 virus. Consistent with the above results, the mice infected with the wild-type CK/A2093 virus underwent only mild body weight loss in the first 3 days post infection and recovered afterward (Fig. 5A). In contrast, all three PB2 mutant viruses caused more severe body weight loss, with the CK/A2093-PB2-double-mut virus ranking first as the infected group suffered rapid and continuous weight reduction that reached 27% at 7 d.p.i., followed by the CK/A2093-PB2-E627K virus and then the CK/A2093-PB2-T473M virus, displaying a nadir weight loss of 18% at 8 d.p.i. and 15% at 6 d.p.i., respectively (Fig. 5A). A similar trend was observed for mortality: the double mutant virus-infected group all died within 8 days post infection whereas 60% of the CK/A2093-PB2-E627K virus-infected group survived at the end of the 14-day

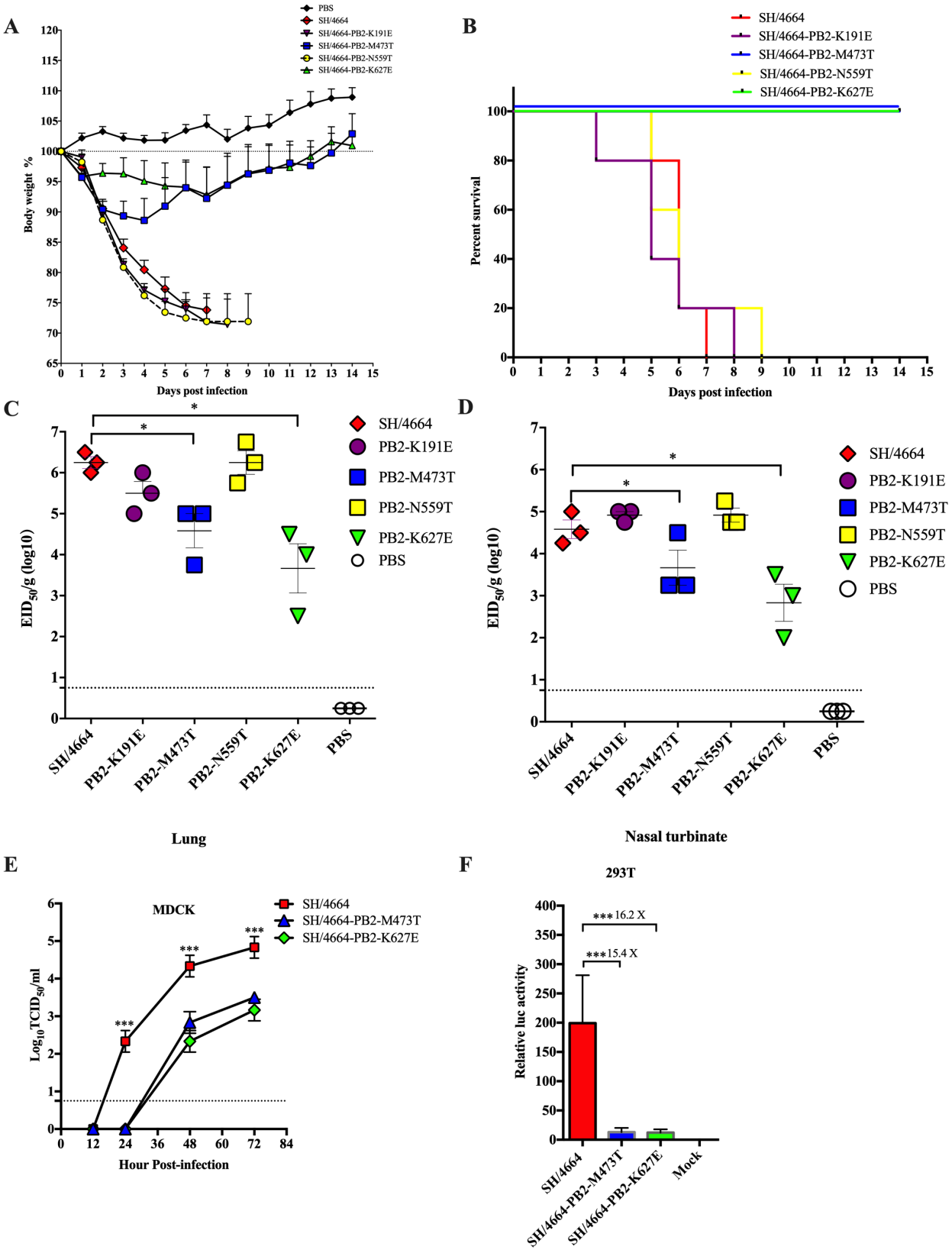

FIG 4 PB2 473M is required for mammalian adaptation of H7N9 AIV due to its essential role in supporting the viral polymerase. SH/4664 PB2 differs from CK/A2093 PB2 in residues 191, 473, 559, and 627. Four recombinant SH/4664 viruses, namely, SH/4664-PB2-K191E, SH/4664-PB2-M473T, SH/4664-PB2-N559T, and

(Continued on next page)

FIG 4 (Continued)

SH/4664-PB2-K627E, were generated by substituting each of these four PB2 residues with that of CK/A2093 PB2. (A–D) The four viruses, along with SH/4664, were used to infect mice at a single dose of 10^6 EID_{50}, followed by determinations of body weight change (A), mortality (B),and viral load in the lung (C) and in the nasal tubinate (D) assessed at 4 d.p.i. (E) Comparison of multiple growth curves of SH/4664, SH/4664-PB2-M473T, and SH/4664-PB2-K627E in cultured Madin-Darby canine kidney (MDCK) cells. Infections were performed at multiplicity of infection (MOI) of 0.001, and supernatants were collected at various time points between 0 and 72 hours post infection for determination of viral titers using 50% tissue culture infectious dose ($TCID_{50}$) assay in MDCK cells. The values displayed are the log_{10} means ± SD from three independent experiments. (F) The effects of PB2 M473T and K627E mutations on viral polymerase activity in 293T cells, assessed by a minigenome assay. Four plasmids respectively expressing PA, PB1, wild-type H7N9 PB2, or its mutant with PB2 M437T or PB2 K627E; NP was co-transfected into 293T cells, together with an influenza-specific Firefly luciferase reporter and a plasmid expressing Renilla luciferase (internal control). Firefly and Renilla luciferase activities were simultaneously measured at 24 hours post transfection. The Firefly luciferase values were normalized to the Renilla luciferase values and expressed as fold inductions over background control (absence of PB2-expressing plasmid). Data represent mean ± SD of three independent experiments. Statistical significance was analyzed using one-way ANOVA. *$P < 0.05$ and ***$P < 0.001$.

observation period. Despite significant weight loss, the CK/A2093-PB2-T473M virus-infected group exhibited a 100% survival rate, the same as the wild-type CK/A2093 virus-infected group (Fig. 5B). We also measured the lung and nasal turbinate viral loads at 3 and 5 d.p.i.. The three PB2 mutant virus-infected groups showed similar higher viral loads compared with the wild-type CK/A2093 virus-infected group at both time points except for lung viral loads of 5 d.p.i., which were likely higher for the double mutant virus-infected group compared with either the single mutant virus-infected group (Fig. 5C and D). Taken together, our analyses of reciprocal SH/4664 mutations at PB2-473 and PB2-627 in the CK/A2093 H9N2 background strengthened the notion that both residues contribute to the mammalian adaptation of AIVs, with PB2-627K appearing to be more influential than PB2-473M.

Chicken ANP32A, but not mouse ANP32A/B, complements influenza viral polymerase with PB2-M473T in human cells

ANP32 family members have been recently identified as host factors connecting with the PB2-627 polymorphism to determine the host range of IAVs (14). While human ANP32A (huANP32A) can only support mammalian-adapted IAV viral polymerase with PB2-627K, chicken ANP32A (chANP32A), with an extra 33-aa insertion compared withs huANP32A, is capable of effectively complementing viral polymerase bearing PB2-627K or the avian signature PB2-627E. Another member of the ANP32 family, ANP32B, has also been implicated in modulating viral polymerase in a host-specific manner, but its working spectrum is somewhat different from that of ANP32A. huANP32A and huANP32B are active in supporting IAV viral polymerase, but chANP32B loses such activity, as does mouse ANP32B (moANP32B). Such activity differences between different ANP32 proteins are attributed to polymorphisms at sites 129/130, which are critical for interaction with the IAV viral polymerase (17, 22, 23).

Given the determining role of ANP32A/B in host restriction of IAV viral polymerase via PB2, we sought to explore the functional relationship between PB2-473 and ANP32 proteins. To this end, we first examined the complementation of PB2-M473T by chANP32A or huANP32A in supporting IAV viral polymerase using a minigenome assay in 293T cells, with wild-type SH/4664 PB2 and PB2-K627E as controls. Consistent with previous studies (15, 16, 24), co-expression of chANP32A could rescue the activity of reconstituted SH/4664 viral polymerase with PB2-627E to a level comparable to that of wild-type SH/4664 viral polymerase (Fig. 6A). Surprisingly, similar enhancement was also observed for the PB2-473T-containing viral polymerase (Fig. 6A). The rescuing effects of chANP32A were not due to altered expression of viral polymerase proteins, as confirmed by western blotting (Fig. 6A). We further tested the multiple cycle growth curve in human A549 lung epithelial cells. Considering that A549 cells are difficult to transfect, we turned to more effective lentiviral transduction for overexpressing chANP32A. To this end, we constructed a chANP32A-expressing lentiviral vector, which also carries a puromycin-resistant marker gene via an IRES element linked to and thus co-expressed with chANP32A from the same transcript. The corresponding lentivirus, alongside the empty

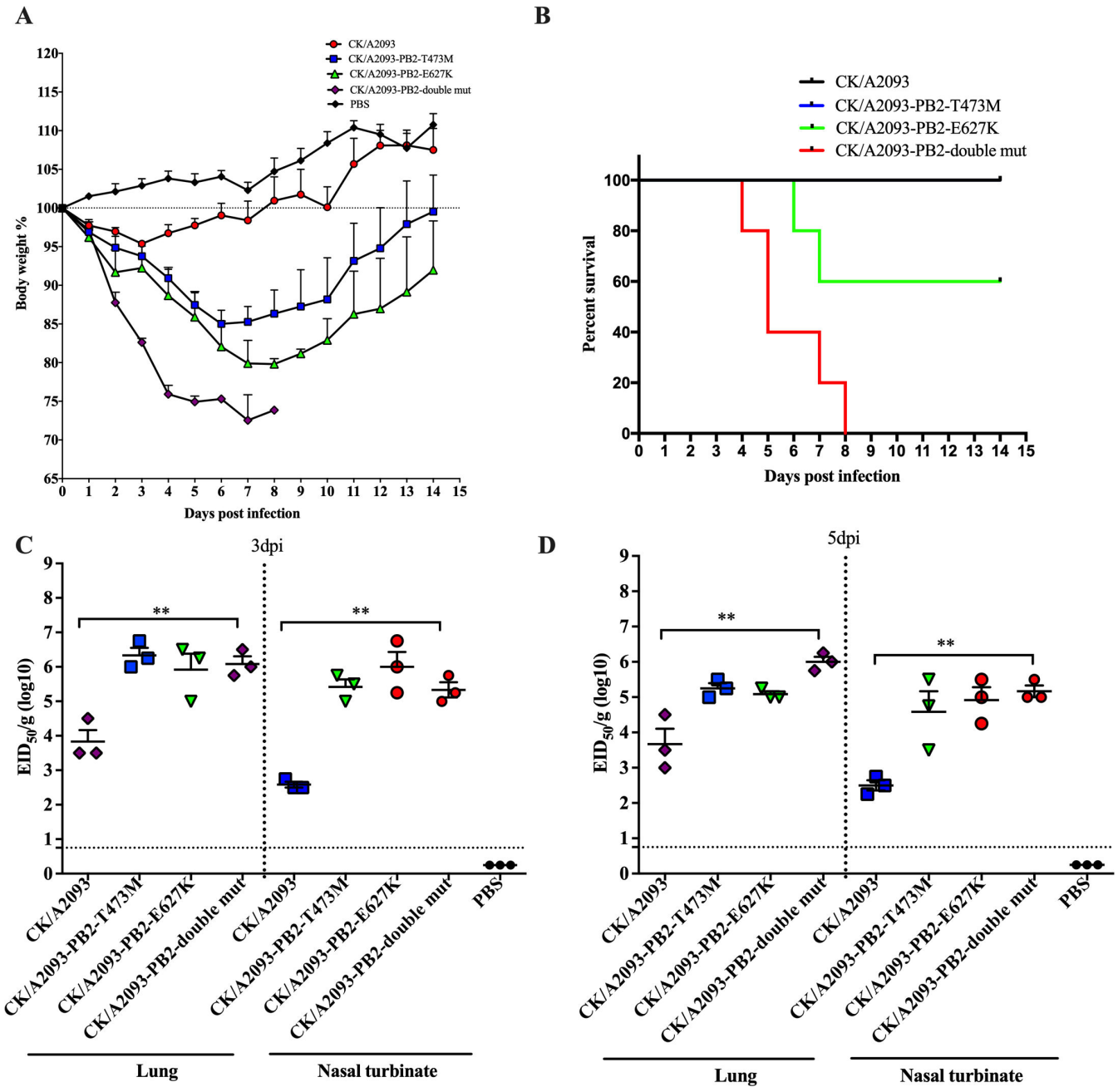

FIG 5 PB2 residues 473 and 627 cooperate in confining the mammalian fitness of the CK/A2093 H9N2 virus. Three CK/A2093 mutant viruses with PB2 residues 473 and 627 individually or simultaneously changed to the corresponding residues of the SH/4664 H7N9 virus, designated as CK/A2093-PB2-E627K, CK/A2093-PB2-T473M, and CK/A2093-PB2-double-mut viruses, were generated and examined in the mouse infection model compared with wild-type CK/A2093, following the same procedures as described in Fig. 1. Shown are (A) body weight change curves, (B)mortality curves, and lung and nasal turbinate $TCID_{50}$ viral titers assessed on 3 d.p.i. (C) and 5 d.p.i. (D). The dashed line indicates the limit of detection of the assay; error bars represent the standard deviations. Statistical significance was analyzed using one-way ANOVA. *$P < 0.05$ and **$P < 0.01$.

control lentivirus, was then produced in 293T cells and used to transduce A549 cells, followed by incubation in puromycin-containing culture medium for selecting successfully transduced cells. The survived cell pools after selection were split and subsequently infected with the wild-type SH/4664 virus, the PB2-M473T mutant virus, or the PB2-K627E mutant virus at a MOI of 0.01. In line with the enhanced viral polymerase activity, multiple cycle growth curve measurements demonstrated that chANP32A-overexpressing A549 cells consistently supported significantly higher levels of viral replication of SH/

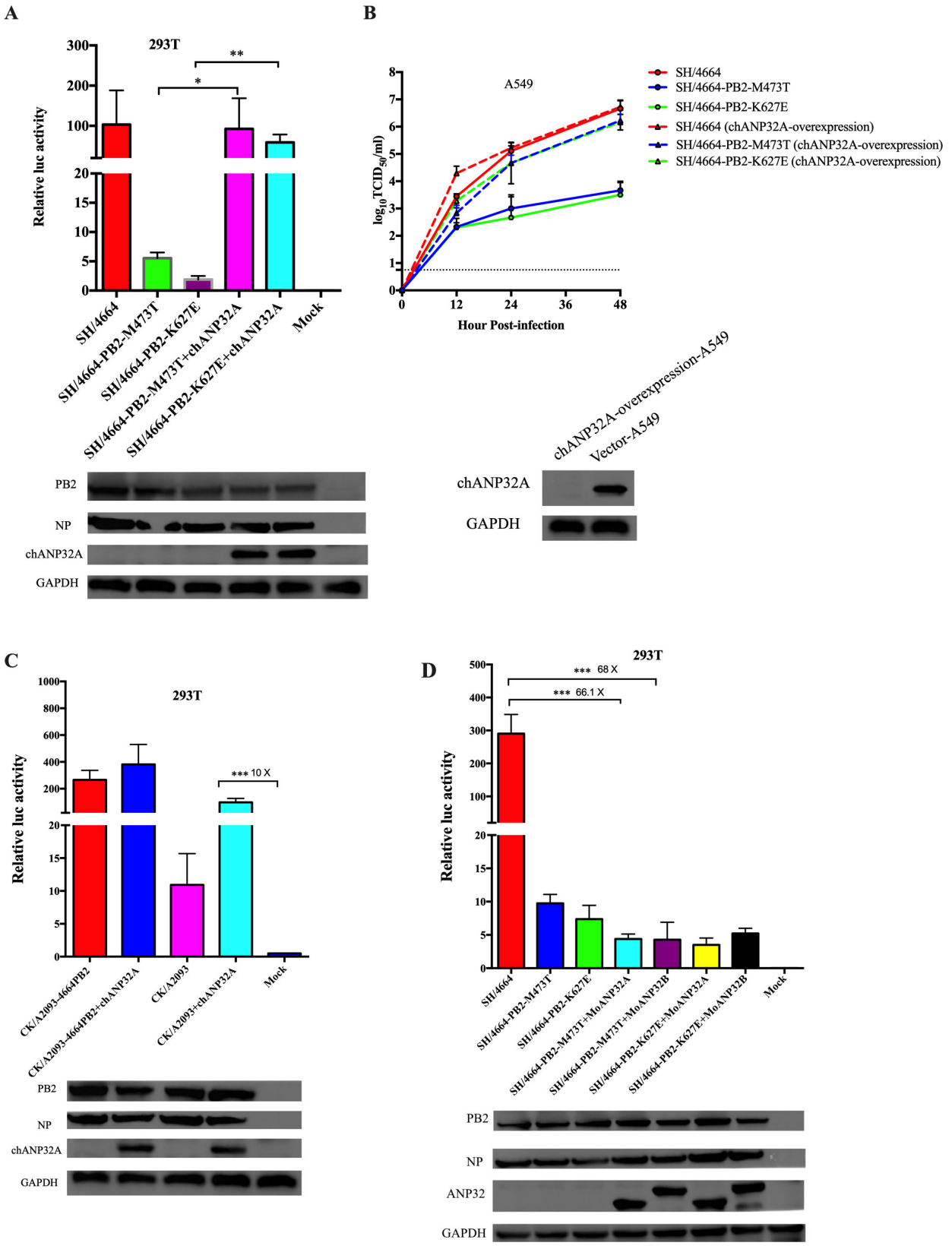

FIG 6 The defective viral polymerase activity associated with PB2 M473T is linked to co-opting of ANP32A host factor. (A) Effects of co-expression of chicken ANP32A (chANP32A) on the activities of reconstituted SH/4664 viral polymerases with PB2 M473T or K627E mutation, examined by minigenome assays. The

(Continued on next page)

FIG 6 (Continued)

minigenome assays in 293T cells were carried out the same as described in Fig. 4F. The cell lysates were also analyzed for expression of PB2 and NP using immunoblotting. Data represent mean ± SD of three independent experiments. (B) Effects of overexpression of chANP32A on multiple growth curves of SH/4664, SH/4664-PB2-M473T, SH/4664-PB2-K627E, and SH/4664 in A549 cells. chANP32A-overexpressing A549 cells, generated by transduction of a lentivirus encoding chANP32A and then selected for the lentivirus-carrying puromycin resistance, were subjected to infection with the wild-type SH/4664 virus or each of the two PB2 mutant viruses at MOI = 0.01, with A549 cells transduced by empty lentivirus as the control. Supernatants were collected at indicated points, and their viral titers were determined by $TCID_{50}$ assays using MDCK cells . The cell lysates were also analyzed for expression of chANP32A using immunoblotting. (C) Complementation of reconstituted CK/A2093 viral polymerase by chANP32A co-expression in minigenome assays in 293T cells. (D) The effects of co-expression of mouse ANP32A (moANP32A) or mouse ANP32B (moANP32B) on the activities of reconstituted SH/4664 viral polymerases with PB2-M473T or PB2-K627E mutation in minigenome assays in 293T cells. Determination of luciferase activities and immunoblotting were performed the same as in A. The relative luciferase activities are presented as mean ± SD of three independent experiments; the viral titers are presented as mean ± SD ($log_{10}TCID_{50}$/mL) of three independent experiments.

4664-PB2-M473T and SH/4664-PB2-K627E mutant viruses compared with control cells; contrastingly, for the wild-type SH/4664 virus, only a moderate difference was observed at an early time point [12 hours post infection (h.p.i.)] (Fig. 6B). Moreover, we found that chANP32A overexpression was also able to complement the CK/A2093 viral polymerase activity in the minigenome assay in 293T cells (Fig. 6C).

Finally, we examined whether mouse ANP32A and ANP32B could support the reconstituted SH/4664 viral polymerase with PB2-K627E or PB2-M473T and found that neither of them conferred a rescuing effect, consistent with the aforementioned mouse infection data (Fig. 6D). Together, these results identified ANP32A as a primary host factor underlying the role of PB2 residue 473 in host adaptation of IAV viral polymerase.

DISCUSSION

H7N9 AIVs have continued to cause human infection since 2013 with high mortality rates. In this study, we explored the mechanism underlying their mammalian adaptation, initiated by comparing in a mouse infection model a series of hybrid virus derived from the SH/4664 H7N9 virus and two H9N2 AIVs. Through this comparison, we pinpointed viral polymerase, then PB2, as the major determinant distinguishing the H7N9 from the H9N2 viruses in mouse virulence. Subsequently, we found that, among the four PB2 residues varying between the SH/4664 H7N9 virus and the closest related CK/A2093 H9N2 virus, 473M and 627K are essential for the SH/4664 virus to replicate effectively in mice, as evidenced by the fact that mouse virulence was abrogated by replacing either residue with the corresponding H9N2 counterpart, namely, M473T or K627E mutations. Corroborating these *in vivo* data, the M473T and K627E mutant viruses showed significant attenuation in cultured mammalian cells, with the corresponding viral polymerase demonstrating markedly reduced activity in the minigenome assay. We further validated the role of PB2-473 and PB2-627 in mammalian fitness of IAVs in the CK/A2093 context. Converting either PB2 residue to the SH/4664 H7N9 counterpart, namely, T473M and E627K, enabled an enhanced virulence, as judged by both weight loss and tissue viral loads. On the other hand, although T473M mutation alone did not result in lethality, it showed an additive or synergistic effect with E627K mutation, as the T473M/E627K double mutant viruses showed more severe weight loss than either single mutant virus and a marked increase in mortality rate from 60% observed for the PB2-627 mutant virus to 100%. Promoting the adaption of viral polymerase to a specific co-factor(s) in the new host has been suggested as a primary mechanism underlying PB2 adaptive mutations. In this respect, we found that the attenuating effect of the M473T mutation on both the H7N9 viral polymerase activity and the H7N9 virus in human cells can be rescued by co-expression of chANP32A, uncovering an unexpected similarity to the K627E mutation. In contrast, mouse ANP32A/ANP32B could not provide such complementation, corroborating the mouse infection results.

Our evaluations of the roles of different gene segments in mouse virulence were carried out in the context of both H7N9 and H9N2 viruses, with opposite effects expected in the two contexts for a given viral gene contributing to the mammalian

adaptation. Unlike PB2, whose critical role in mouse virulence was revealed in both H7N9 and H9N2 contexts by all the used assessments, we observed a context-dependent contribution of PA and NP that only affects specific aspect(s) of mouse virulence. For example, exchanging NP between SH/4664 and CK/F98 appeared to impact pathogenicity more significantly on the CK/F98 side than on the SH/4664 side, as judged by weight loss. Such context dependency suggested that the contribution of NP to mammalian adaption might be at least partially influenced by the viral polymerases. Previous studies implicated the provision of MX resistance as a mechanism underlying adaptive NP mutations (4, 25–28). This mechanism doesn't account for the observed enhancement of mouse virulence conferred by SH4664 NP in the CK/F98 background, as infections were carried out with MX1-negative BALB/c mice. Of interest, one recent study demonstrated that ANP32 mediates the recruitment of NP by IAV viral polymerase besides stabilizing polymerase dimerization (29). This finding raises the possibility that the co-opting of ANP32 might represent a common theme underlying mammalian adaptation driven by NP and viral polymerase, which awaits further investigation.

The most intriguing result of our study is showing the linkage of PB2-473 to species-specific usage of ANP32A. Structurally, residue 473 is part of a β-sheet located at the end of the cap-binding domain of PB2 (30) and exposed in the structure of the viral polymerase in apo or transcription pre-initiation form. Despite the exposure nature of PB2-473M, it is spatially distant from the 627 domain in both forms of the viral polymerase. Carrique et al. recently reported cryo-EM structures of complexes formed by influenza C virus polymerase (FluPolC) and huANP32A or chANP32A (31). The two structures, surprisingly largely identical, revealed the involvement of both LRR and LCAR domains in the binding of ANP32A to FluPolC. For both huANP32A and chANP32A, the LRR domain is positioned between and thus bridges a vRNA-bound FluPolC molecule [FluPol replicase ($FluPol_R$)] and a free FluPolC molecule [encapsidating FluPol ($FluPol_E$)] (31). In contrast, the landscape of PB2 interactions mediated by the LCAR domain varies between chANP32A and huANP32A: chANP32A, owing to its unique 33-aa insertion, uses a stretch of mixed basic and acidic residues to bind to a basic groove of the PB2 627 domain, whereas the corresponding sequence in huANP32A is entirely acidic, rendering it incompatible with 627E-type viral polymerase. Other sequences of the 33-aa insertion might also contribute to the plasticity of chANP2A in accommodate 627K- or 627E-type viral polymerase by providing additional contacts to strengthen the interaction with the PB2 627 domain (31). These structures support the model that PB2-ANP32A interaction facilitates the assembly of influenza virus replicase, consistent with the observation that ANP32A regulates only viral genome replication but not transcription. However, this structural revelation still has limitations. First, given the sequence divergence between FluPolC and FluPolA, to what extent the model is applicable to the FluPolA-ANP32 interaction remains unknown. Second, the interface between the ANP32A LCAR domain and the PB2 627 domain is determined based on continuous density rather than unambiguous mapping. A recent NMR-based study also unravels direct interactions between ANP32A and the PB2 627 domain. Unfortunately, it used the isolated PB2 627 domains instead of the viral polymerases (32).

Although the currently available structures of ANP32A-PB2, as discussed above, did not reveal a direct involvement of residue 473 in the PB2's binding to ANP32A, a previous study predicted PB2 473M as a key huANP32-interacting residue (33). This prediction, based on molecular docking simulation of the PB2-huANP32A interaction, was corroborated by yeast two-hybrid assays detecting an interaction between the LCAR domain of huANP32A and a PB2 fragment spanning residues 307–534 (33). Given that the LCAR domain of ANP32A has not been fully structurally resolved, indicative of a highly dynamic nature, it is plausible to speculate that, in the case of huANP32A, its optimal co-opting by FluPolA requires the LCAR domain to interact with both 627K and 473M of PB2. This speculation aligns with our observations made with recombinant viruses of CK/A2093 background that the PB2 T473M-K627E double mutant virus was more virulent than the two single mutant viruses, as reflected in mortality rate and

weight loss. The PB2 473M and 627K dependency of AIVs is relieved in avian cells, as the extra 33-aa insertion of chANP32A allows tolerance of polymorphism at the two positions. Notably, an alternative hypothesis of PB2 627-mediated ANP32A adaptation has been proposed to explain the observation that PB2-627K and PB2-627E showed similar weak binding to huANP32A, while only the former is capable of supporting high viral polymerase activity in mammalian cells, that is, PB2-627K enables more efficient use of huANP32A than PB2-627E without affecting the interaction with huANP32A *per se*. This view implies that ANP32 proteins may have an expanding role in regulating FluPolA activity beyond promoting its dimerization, and it has received support from a recent finding that ANP32 proteins interact with NP and facilitate its recruitment during viral RNA replication (29). Thus, PB2 473 could alternatively impact the co-opting of mammalian ANP32 by FluPolA at the exploitation step after its recruitment. It should be noted that diverse mammalian adaptation-related PB2 mutations other than PB2 E627K, exemplified by the D701N mutation once thought to be driven by adaptation to host importin proteins, were recently found to be capable of enhancing the complementation of FluPolA activity by huANP32A/huANP32B (34). Further elucidation of how ANP32 proteins regulate the IAV vRNP-directed viral RNA synthesis, as well as in which state the vPol favors the recruitment and/or exploitation of ANP32 proteins, would be essential for understanding the broad connection of ANP32 to different constellations of PB2 adaptive mutations. Along this line, it would be particularly beneficial if the structure of the ANP32-FluPolA-NP complex could be solved.

It is noteworthy that the connection of PB2 473 to mammalian adaptation had previously been suggested for H5N1 AIVs (35). However, the subsequent mutation analyses found that substituting PB2 473M with leucine (L), the counterpart residue in the H5N1 strain, had little effect on the H5N1 viral polymerase activity (35). We observed a similar non-significant impact of the PB2 M473L alteration on the SH/4664 viral polymerase activity in the minigenome assay (unpublished data). Thus, it appeared that L but not T is tolerated at position 473 for the fitness of AIV vPol in mammalian cells. Interestingly, PB2 473M has a dominant presence in all subtypes of IAVs, irrespective of origin. For example, PB2 of the other H9N2 virus used in the study, the CK/F98 virus, contains 31 residues different from SH/4664 H7N9 PB2, including 627E, but retains 473M. Our discovery of the importance of PB2 473 in mammalian adaptation of AIVs is attributed to choosing CK/A2093 H9N2 PB2 as the comparison counterpart of SH/4664 H7N9 PB2. The selection mechanism underlying the dominance of PB2 473M for AIVs without mammalian adaptation requires future investigation.

In conclusion, we identified PB2-473, in both contexts of a human-adapted H7N9 virus and its H9N2 counterpart, as a new determinant for the virulence of AIVs in mice. We further demonstrated that this residue, spatially separated from the PB2 627 domain, is functionally linked to the ANP32A host factor in influencing viral polymerase activity. Our study provides new insight into how PB2 co-opts ANP32 to set the host ranges of IAVs.

MATERIALS AND METHODS

Viruses and cells

A/Chicken/Shanghai/F/98 (CK/F98) and A/Chicken/shanghai/A2093/2011 (CK/A2093) H9N2 avian influenza virus were provided by Dr. Zejun Li (Shanghai Veterinary Research Institute, CAAS). H7N9 virus A/Shanghai2/4664T/2013 (SH/4664) was conserved at biosafety level 3 lab at Shanghai Public Clinical Center. All the recombinant viruses were generated by an eight-plasmid reverse genetics system as described previously (21). The recombinant viruses were verified by sequencing all the eight segments using Sanger method (TSINGKE, Shanghai, China). Virus stocks were propagated in 9-day-old SPF embryonated chicken eggs incubated at 37°C; EID_{50} titers and $TCID_{50}$ were determined in chicken eggs and MDCK cells, respectively, according to the Reed-Muench method.

MDCK cells and 293T cells were purchased from American Type Culture Collection (ATCC) and maintained at 37C, 5% CO2 in Dulbecco's modified Eagle's medium (Corning) supplemented with 10% fetal calf serum (Biosera) and 1% penicillin-streptomycin (New Cell & Molecular Biotech, C100C5)

Assaying virus replication in MDCK cells

MDCK cells were infected with the indicated viruses at a MOI of 0.001. Following 1-hour adsorption at 37°C, the unabsorbed viruses were removed. The cells were washed three times with PBS buffer and then incubated in fresh OPTI-MEM medium supplemented with 1 µg mL^{-1} N-acetylated trypsin (TPCK-trypsin) at 37°C, 5% CO_2. Culture supernatants were collected at various time points post infection, and $TCID_{50}$ virus titers were determined in MDCK cells.

Animal infections

Five- to 6-week-old female Balb/c mice (Vital River Co., Beijing) were anesthetized with pentobarbital and then intranasally inoculated with $1 \times 10_6$ EID_{50} of the indicated virus in a volume of 50 µL (11 mice per group). An additional five mice were inoculated with 50 µL PBS buffer, serving as mock controls. The weight change and mortality were monitored daily for up to 14 days. Mice were scored dead and humanely euthanized if they lost more than 25% of their initial body weights. For assessing viral replication, three mice in each group were sacrificed on days 3–5 post infection to collect lungs and nasal turbinates for viral load determination as previously described (36). In brief, the tissues were weighted and mixed with 10 mM PBS at 1 g/mL (wt/vol), and homogenates were made with 2-mm tungsten carbide beads by oscillating 70 times at 1/s for 2 min in a Tissue Lyser apparatus (Qiagen Tissue Lyser II). The resulting homogenates were cleared by centrifugation at 12,000 rpm for 10 minutes, and then, serial 1:10 dilutions were prepared and inoculated into 9-day-old embryonated eggs with 100 µL per egg. Titers were calculated using the Reed-Muench method and expressed as mean $\log_{10}$ EID_{50}/g ± SD, with the limit of detection set at 0.75 $\log_{10}$ EID_{50}/g.

Minigenome reporter assays

Transfections were performed with the TransT-293 transfection reagent (Mirus, MIR 2706), following the manufacturer's protocol. 293T cells were seeded 1 day prior to transfection and transfected at 60%–80% confluency with a plasmid mix containing (i) 100 ng each of the pCAGGS plasmids expressing PA, PB1, PB2, or its mutant carrying M473E or K627 mutation and or NP; (ii) 20 ng of a reporter plasmid encoding the Firefly luciferase gene flanked by the 5′ UTR and 3′ UTR of the influenza A/WSN/33 NP segment; and (iii) 20 ng of a plasmid constitutively expressing Renilla luciferase, serving as an internal control to monitor transfection efficiency. Transfected cells were incubated at 37°C, 5% CO_2 for an additional 24 hours, and then harvested to make lysates subjected to determinations of both Firefly and Renilla luciferase activities using a Dual-Luciferase Reporter Assay System (Promega) and a microplate reader. The Firefly luciferase data were normalized to the Renilla luciferase data. In assays involving co-expression of chANP32A, huANP32A, mouse ANP32A, or mouse ANP32B, 100 ng of a corresponding pCAGGS-based expression plasmid expressing chANP32A was added to the plasmid mix.

Complementation of PB2 mutant viruses in human cells by chANP32A

The experiments were performed in A549 cells. chANP32A overexpression was achieved in A549 cells by transduction of a chANP32A-expressing lentivirus. The lentiviral vector expressing chANP32A, pHAGE-CMV-chANP32A-IRES-Puro, was constructed by cloning the coding sequence of chANP32A into the pHAGE vector (Addgene), enabling its co-expression with the downstream puromycin-resistant marker gene in an IRES-dependent manner. The pHAGE-CMV-chANP32A-IRES-Puro or empty pHAGE lentiviral vector was then used to co-transfect 293T cells with two viral packaging plasmids,

pMD2.G and psPAX2 (Addgene), for lentivirus production. Supernatants were harvested 48 hours post transfection as lentivirus stocks and used to transduce A549 cells, followed by selection with puromycin (2 µg/mL) starting 2 days later and lasting 7 days. The surviving cells were replated and subsequently subjected to infection with the indicated IAVs. IAV infection and growth curve determination with A549 cells were performed following the same procedures as described above for MDCK cells, except for increasing the MOI to 0.01 and decreasing the concentration of N-acetylated trypsin (NAT) in the medium to 0.2 µg/mL during the incubation period post infection.

Statistical analysis

All the statistical analyses were conducted using the Prism 7 software (GraphPad, La Jolla, CA). Differences between two groups were analyzed by two-tailed Student's *t*-test, whereas comparisons of means across more than two groups were performed using one-way ANOVA.

ACKNOWLEDGMENTS

We thank our colleagues Songhua Yuan, Longfei Ding, Qian He, and Linxia Zhang for their contribution in mouse sample processing.

This work was supported by the National Key R&D Program of China (2022YFC2604100), the Lancang-Mekong Countries Animal Biosafety Prevention and Control Cooperation (125161035), the National Natural Science Foundation of China (82072273), and the intramural Funding from Shanghai Public Health Clinical Center (to M.Z.).

AUTHOR AFFILIATIONS

[1]Shanghai Public Health Clinical Center, Fudan University, Shanghai, China
[2]Shanghai Veterinary Research Institute, Shanghai, China
[3]Zhongshan Hospital, Institutes of Biomedical Sciences, Fudan University, Shanghai, China
[4]Academy for Advanced Interdisciplinary Studies, Peking University, Beijing, China

AUTHOR ORCIDs

Miaomiao Zhang http://orcid.org/0000-0003-4657-5320
Chen Zhao http://orcid.org/0000-0002-0718-7707
Jianqing Xu http://orcid.org/0000-0003-0896-9273
Zejun Li http://orcid.org/0000-0003-4368-1988
Xiaoyan Zhang http://orcid.org/0000-0002-3193-1401

AUTHOR CONTRIBUTIONS

Miaomiao Zhang, Data curation, Formal analysis, Methodology, Software, Visualization, Writing – original draft | Mingbin Liu, Methodology | Hongjun Chen, Formal analysis | Tianyi Qiu, Software | Weihui Fu, Visualization | Chen Zhao, Investigation, Resources, Writing – review and editing | Jianqing Xu, Formal analysis, Funding acquisition, Supervision | Zejun Li, Conceptualization, Data curation, Funding acquisition, Project administration, Supervision | Xiaoyan Zhang, Funding acquisition, Resources, Supervision.

DATA AVAILABILITY

The data used to support the findings of this study are available from the corresponding author upon request.

ETHICS APPROVAL

All animal studies were conducted in accordance with the "Guide for the Care and Use of Laboratory Animals of the Institute of Laboratory Animal Science (est. 2006)." The experiments involving live viruses were carried out in a biosafety level 3 (BSL3) facility at Shanghai Public Clinical Center, Fudan University, conforming to protocols approved by the Institutional Biosafety Committee at Shanghai Public Health Clinical Center.

ADDITIONAL FILES

The following material is available online.

Supplemental Material

Fig. S1 (JVI01944-23-s0001.tiff). Validation of the attenuated mouse virulence of the SH/4664 virus by PB2-M473T or PB2-K627E mutation.
Fig. S2 (JVI01944-23-s0002.tiff). Uncropped Western blot images for Fig. 6A to D.
Supplemental legends (JVI01944-23-s0003.docx). Legends for Fig. S1 and S2.

REFERENCES

1. Zhou J, Wang D, Gao R, Zhao B, Song J, Qi X, Zhang Y, Shi Y, Yang L, Zhu W, et al. 2013. Biological features of novel avian influenza A (H7N9) virus. Nature 499:500–503. https://doi.org/10.1038/nature12379
2. Gao R, Cao B, Hu Y, Feng Z, Wang D, Hu W, Chen J, Jie Z, Qiu H, Xu K, et al. 2013. Human infection with a novel avian-origin influenza A (H7N9) virus. N Engl J Med 368:1888–1897. https://doi.org/10.1056/NEJMoa1304459
3. Shinya K, Ebina M, Yamada S, Ono M, Kasai N, Kawaoka Y. 2006. Avian flu: influenza virus receptors in the human airway. Nature 440:435–436. https://doi.org/10.1038/440435a
4. Long JS, Mistry B, Haslam SM, Barclay WS. 2019. Host and viral determinants of influenza A virus species specificity. Nat Rev Microbiol 17:67–81. https://doi.org/10.1038/s41579-018-0115-z
5. Shi Y, Zhang W, Wang F, Qi J, Wu Y, Song H, Gao F, Bi Y, Zhang Y, Fan Z, Qin C, Sun H, Liu J, Haywood J, Liu W, Gong W, Wang D, Shu Y, Wang Y, Yan J, Gao GF. 2013. Structures and receptor binding of hemagglutinins from human-infecting H7N9 influenza viruses. Science 342:243–247. https://doi.org/10.1126/science.1242917
6. Li Q, Zhou L, Zhou M, Chen Z, Li F, Wu H, Xiang N, Chen E, Tang F, Wang D, et al. 2014. Epidemiology of human infections with avian influenza A(H7N9) virus in China. N Engl J Med 370:520–532. https://doi.org/10.1056/NEJMoa1304617
7. Subbarao EK, London W, Murphy BR. 1993. A single amino acid in the PB2 gene of influenza A virus is a determinant of host range. J Virol 67:1761–1764. https://doi.org/10.1128/JVI.67.4.1761-1764.1993
8. Chen H, Yuan H, Gao R, Zhang J, Wang D, Xiong Y, Fan G, Yang F, Li X, Zhou J, et al. 2014. Clinical and epidemiological characteristics of a fatal case of avian influenza A H10N8 virus infection: a descriptive study. Lancet 383:714–721. https://doi.org/10.1016/S0140-6736(14)60111-2
9. Gao Z, Bao J. 2014. Inspiration and challenge of facing human infection with the H7N9 avian influenza. Zhonghua Jie He He Hu Xi Za Zhi 37:4–5.
10. Gabriel G, Dauber B, Wolff T, Planz O, Klenk HD, Stech J. 2005. The viral polymerase mediates adaptation of an avian influenza virus to a mammalian host. Proc Natl Acad Sci U S A 102:18590–18595. https://doi.org/10.1073/pnas.0507415102
11. Li Z, Chen H, Jiao P, Deng G, Tian G, Li Y, Hoffmann E, Webster RG, Matsuoka Y, Yu K. 2005. Molecular basis of replication of duck H5N1 influenza viruses in a mammalian mouse model. J Virol 79:12058–12064. https://doi.org/10.1128/JVI.79.18.12058-12064.2005
12. Song W, Wang P, Mok B-Y, Lau S-Y, Huang X, Wu W-L, Zheng M, Wen X, Yang S, Chen Y, Li L, Yuen K-Y, Chen H. 2014. The K526R substitution in viral protein PB2 enhances the effects of E627K on influenza virus replication. Nat Commun 5:5509. https://doi.org/10.1038/ncomms6509
13. Wang C, Lee HHY, Yang ZF, Mok CKP, Zhang Z. 2016. PB2-Q591K mutation determines the pathogenicity of avian H9N2 influenza viruses for mammalian species. PLoS ONE 11:e0162163. https://doi.org/10.1371/journal.pone.0162163
14. Long JS, Giotis ES, Moncorgé O, Frise R, Mistry B, James J, Morisson M, Iqbal M, Vignal A, Skinner MA, Barclay WS. 2016. Species difference in ANP32A underlies influenza A virus polymerase host restriction. Nature 529:101–104. https://doi.org/10.1038/nature16474
15. Baker SF, Ledwith MP, Mehle A. 2018. Differential splicing of ANP32A in birds alters its ability to stimulate RNA synthesis by restricted influenza polymerase. Cell Rep 24:2581–2588. https://doi.org/10.1016/j.celrep.2018.08.012
16. Domingues P, Hale BG. 2017. Functional insights into ANP32A-dependent influenza A virus polymerase host restriction. Cell Rep 20:2538–2546. https://doi.org/10.1016/j.celrep.2017.08.061
17. Zhang H, Zhang Z, Wang Y, Wang M, Wang X, Zhang X, Ji S, Du C, Chen H, Wang X. 2019. Fundamental contribution and host range determination of ANP32A and ANP32B in influenza A virus polymerase activity. J Virol 93:e00174-19. https://doi.org/10.1128/JVI.00174-19
18. Domingues P, Eletto D, Magnus C, Turkington HL, Schmutz S, Zagordi O, Lenk M, Beer M, Stertz S, Hale BG. 2019. Profiling host ANP32A splicing landscapes to predict influenza A virus polymerase adaptation. Nat Commun 10:3396. https://doi.org/10.1038/s41467-019-11388-2
19. Zhang H, Li H, Wang W, Wang Y, Han GZ, Chen H, Wang X. 2020. A unique feature of swine ANP32A provides susceptibility to avian influenza virus infection in pigs. PLoS Pathog 16:e1008330. https://doi.org/10.1371/journal.ppat.1008330
20. Thiele S, Stanelle-Bertram S, Beck S, Kouassi NM, Zickler M, Müller M, Tuku B, Resa-Infante P, van Riel D, Alawi M, Günther T, Rother F, Hügel S, Reimering S, McHardy A, Grundhoff A, Brune W, Osterhaus A, Bader M, Hartmann E, Gabriel G. 2020. Cellular importin-α3 expression dynamics in the lung regulate antiviral response pathways against influenza A virus infection. Cell Rep 31:107549. https://doi.org/10.1016/j.celrep.2020.107549
21. Zhang M, Zhao C, Chen H, Teng Q, Jiang L, Feng D, Li X, Yuan S, Xu J, Zhang X, Li Z. 2020. Internal gene cassette from a human-origin H7N9 influenza virus promotes the pathogenicity of H9N2 avian influenza virus in mice. Front Microbiol 11:1441. https://doi.org/10.3389/fmicb.2020.01441
22. Mistry B, Long JS, Schreyer J, Staller E, Sanchez-David RY, Barclay WS. 2020. Elucidating the interactions between influenza virus polymerase and host factor ANP32A. J Virol 94:e01353-19. https://doi.org/10.1128/JVI.01353-19
23. Staller E, Sheppard CM, Neasham PJ, Mistry B, Peacock TP, Goldhill DH, Long JS, Barclay WS. 2019. ANP32 proteins are essential for influenza virus replication in human cells. J Virol 93:e00217-19. https://doi.org/10.1128/JVI.00217-19
24. Long JS, Giotis ES, Moncorgé O, Frise R, Mistry B, James J, Morisson M, Iqbal M, Vignal A, Skinner MA, Barclay WS. 2016. Species difference in

ANP32A underlies influenza A virus polymerase host restriction. Nature 529:101–104. https://doi.org/10.1038/nature16474
25. Mänz B, Dornfeld D, Götz V, Zell R, Zimmermann P, Haller O, Kochs G, Schwemmle M. 2013. Pandemic influenza A viruses escape from restriction by human MxA through adaptive mutations in the nucleoprotein. PLoS Pathog 9:e1003279. https://doi.org/10.1371/journal.ppat.1003279
26. Ashenberg O, Padmakumar J, Doud MB, Bloom JD. 2017. Deep mutational scanning identifies sites in influenza nucleoprotein that affect viral inhibition by MxA. PLoS Pathog 13:e1006288. https://doi.org/10.1371/journal.ppat.1006288
27. Deeg CM, Hassan E, Mutz P, Rheinemann L, Götz V, Magar L, Schilling M, Kallfass C, Nürnberger C, Soubies S, Kochs G, Haller O, Schwemmle M, Staeheli P. 2017. *In vivo* evasion of MxA by avian influenza viruses requires human signature in the viral nucleoprotein. J Exp Med 214:1239–1248. https://doi.org/10.1084/jem.20161033
28. Riegger D, Hai R, Dornfeld D, Mänz B, Leyva-Grado V, Sánchez-Aparicio MT, Albrecht RA, Palese P, Haller O, Schwemmle M, García-Sastre A, Kochs G, Schmolke M. 2015. The nucleoprotein of newly emerged H7N9 influenza A virus harbors a unique motif conferring resistance to antiviral human MxA. J Virol 89:2241–2252. https://doi.org/10.1128/JVI.02406-14
29. Wang F, Sheppard CM, Mistry B, Staller E, Barclay WS, Grimes JM, Fodor E, Fan H. 2022. The C-terminal LCAR of host ANP32 proteins interacts with the influenza A virus nucleoprotein to promote the replication of the viral RNA genome. Nucleic Acids Res 50:5713–5725. https://doi.org/10.1093/nar/gkac410
30. Guilligay D, Tarendeau F, Resa-Infante P, Coloma R, Crepin T, Sehr P, Lewis J, Ruigrok RWH, Ortin J, Hart DJ, Cusack S. 2008. The structural basis for cap binding by influenza virus polymerase subunit PB2. Nat Struct Mol Biol 15:500–506. https://doi.org/10.1038/nsmb.1421
31. Carrique L, Fan H, Walker AP, Keown JR, Sharps J, Staller E, Barclay WS, Fodor E, Grimes JM. 2020. Host ANP32A mediates the assembly of the influenza virus replicase. Nature 587:638–643. https://doi.org/10.1038/s41586-020-2927-z
32. Camacho-Zarco AR, Kalayil S, Maurin D, Salvi N, Delaforge E, Milles S, Jensen MR, Hart DJ, Cusack S, Blackledge M. 2020. Molecular basis of host-adaptation interactions between influenza virus polymerase PB2 subunit and ANP32A. Nat Commun 11:3656. https://doi.org/10.1038/s41467-020-17407-x
33. Wei X, Liu Z, Wang J, Yang R, Yang J, Guo Y, Tan H, Chen H, Liu Q, Liu L. 2019. The interaction of cellular protein ANP32A with influenza A virus polymerase component PB2 promotes vRNA synthesis. Arch Virol 164:787–798. https://doi.org/10.1007/s00705-018-04139-z
34. Peacock TP, Sheppard CM, Lister MG, Staller E, Frise R, Swann OC, Goldhill DH, Long JS, Barclay WS. 2023. Mammalian ANP32A and ANP32B proteins drive differential polymerase adaptations in avian influenza virus. J Virol 97:e0021323. https://doi.org/10.1128/jvi.00213-23
35. Fan S, Hatta M, Kim JH, Halfmann P, Imai M, Macken CA, Le MQ, Nguyen T, Neumann G, Kawaoka Y. 2014. Novel residues in avian influenza virus PB2 protein affect virulence in mammalian hosts. Nat Commun 5:5021. https://doi.org/10.1038/ncomms6021
36. Zhang M, Zhang X, Xu K, Teng Q, Liu Q, Li X, Yang J, Xu J, Chen H, Zhang X, Li Z. 2016. Characterization of the pathogenesis of H10N3, H10N7, and H10N8 subtype avian influenza viruses circulating in ducks. Sci Rep 6:34489. https://doi.org/10.1038/srep34489